Available online at www.sciencedirect.com
ScienceDirect
International Journal of Non-Linear Mechanics 43 (2008) 140–149
INTERNATIONAL JOURNAL OF NON-LINEAR MECHANICS
www.elsevier.com/locate/nlm

Criticality of Hopf bifurcation in state-dependent delay model of turning processes

Tamás Insperger[a,*], David A.W. Barton[b], Gábor Stépán[a]

[a]Department of Applied Mechanics, Budapest University of Technology and Economics, H-1521 Budapest, Hungary
[b]Department of Engineering Mathematics, University of Bristol, Bristol, UK

Received 17 July 2007; received in revised form 6 November 2007; accepted 6 November 2007

Abstract

In this paper the non-linear dynamics of a state-dependent delay model of the turning process is analyzed. The size of the regenerative delay is determined not only by the rotation of the workpiece, but also by the vibrations of the tool. A numerical continuation technique is developed that can be used to follow the periodic orbits of a system with implicitly defined state-dependent delays. The numerical analysis of the model reveals that the criticality of the Hopf bifurcation depends on the feed rate. This is in contrast to simpler constant delay models where the criticality does not change. For small feed rates, subcritical Hopf bifurcations are found, similar to the constant delay models. In this case, periodic orbits coexist with the stable stationary cutting state and so there is the potential for large amplitude chatter and bistability. For large feed rates, the Hopf bifurcation becomes supercritical for a range of spindle speeds. In this case, stable periodic orbits instead coexist with the unstable stationary cutting state, removing the possibility of large amplitude chatter. Thus, the state-dependent delay in the model has a kind of stabilizing effect, since the supercritical case is more favorable from a practical viewpoint than the subcritical one.

Keywords: Machine tool chatter; State-dependent delay; Hopf bifurcation

1. Introduction

Delay-differential equations (DDEs) often arise in many different fields of science and engineering; examples include control systems [1], lasers [2] and neuroscience [3]. One relevant mechanical application is the dynamics of cutting processes. The first mechanical models of cutting processes appeared in the works of Tlusty [4] and Tobias [5]. These models describe the machine tool/workpiece structure as a flexible system, where the tool and/or the workpiece experience vibrations. These vibrations cause variations in the cutting depth and so in the next revolution of the workpiece the tool encounters the wavy surface that was created. Due to this regeneration effect, the chip thickness (and hence cutting force) is determined by the current and previous positions of the tool and the workpiece. In the standard models appearing in the literature the time delay between two successive cuts is considered to be a constant, which is equal to the period of the workpiece rotation for turning, and to the tooth passing period for milling. The corresponding mathematical model of the turning process is an autonomous DDE, while the milling operation can be described by DDEs with time-periodic coefficients.

An important phenomenon that limits the productivity of machining is the onset of self-excited vibrations, also known as machine tool chatter. Typically, these vibrations are associated with subcritical Hopf bifurcations. The locations of these Hopf bifurcations of machining processes are usually shown in the form of stability lobe diagrams. These diagrams plot the stable axial cutting depth as function of the spindle speed. Since DDEs have infinite dimensional state-spaces [6–8], closed form stability criteria are not usually available. However, there exist several numerical and semi-analytical techniques to construct stability diagrams (see, e.g., [8–12]).

Models with constant time delay capture the main character of regenerative dynamics and can be used to describe linear

* Corresponding author. Tel.: +36 01 463 1227; fax: +36 01 463 3471.
E-mail addresses: inspi@mm.bme.hu (T. Insperger), david.barton@bristol.ac.uk (D.A.W. Barton), stepan@mm.bme.hu (G. Stépán).

0020-7462/$ - see front matter © 2007 Elsevier Ltd. All rights reserved.
doi:10.1016/j.ijnonlinmec.2007.11.002

stability properties in good agreement with experiments. However, some phenomena can only be explained using more sophisticated models that incorporate varying time delay as well. Accurate modeling of milling operations shows that the regenerative delay is in fact time periodic due to the feed motion, and the corresponding stability diagrams differ from the ones of traditional models with constant delay (see [13–15]).

If the regenerative process is to be modeled accurately, then the vibrations of the tool should also be included in the time delay. In turning processes, the time delay is basically determined by the rotation of the workpiece but it is also affected by the current and the delayed position of the tool as it was shown by Insperger et al. [16,17]. This results in a DDE with state-dependent delay (SD-DDE) where the delay depends on the present state and also on a delayed one, thus giving an implicitly defined delay. The effect of state-dependent delay is also important in rotary cutting processes (e.g., in milling, or drilling) where the torsional vibrations of the tool are significant in the system's dynamics. Germay et al. [18] and Richard et al. [19] investigated drilling with drag bits and showed that state-dependent regenerative delay arises due to the torsional vibration of the tool. Insperger et al. [20] showed that state-dependent delay arises in the governing equation of the milling process even when only the bending oscillation of the tool is considered and its torsional compliance is neglected.

The theory of SD-DDEs is an actively developing research area in mathematics (see, e.g., [21–25]) and results, like linearization techniques and stability analysis, are not used in engineering problems yet. SD-DDEs are always non-linear, since the state itself arises in its own argument through the delay. The linearized system, however, is a DDE with constant (or time-dependent) delay. Linearization of SD-DDEs is complicated by the fact that the solution of the system is not differentiable with respect to the state-dependent delay. Consequently, "true" linearization is not possible, rather we are looking for a linear DDE, which is associated to the original system in the sense that they have the same local stability properties.

Linear stability analysis of the state-dependent delay model of turning process was given in [17] using the technique of Hartung and Turi [22]. In the current paper, the nonlinear behavior of the same model is analyzed using numerical continuation techniques.

For turning models with constant delay, subcritical Hopf bifurcations occur, i.e., unstable periodic orbits coexist with the stable stationary cutting below the stability lobes. This means that chatter may arise in the cases where the system is linearly stable. This phenomenon was clearly shown experimentally by Shi and Tobias [26]. The first mechanical model that provided analytical explanation of the unstable limit cycle was presented by Stépán and Kalmár-Nagy [27]. Since then, their results were confirmed by different numerical techniques (see, e.g., [28–32]).

In this paper, it is shown that the Hopf bifurcation may in fact become supercritical for some parameter values if a state-dependent regenerative delay is incorporated into the model. In these cases, small amplitude stable periodic orbits coexist with the unstable stationary cutting solution above the stability lobes, and no periodic orbits coexist with the stable stationary cutting. This is practically more favorable than the subcritical case since chatter cannot occur below the stability lobes. The results are obtained by a numerical continuation technique.

2. Mechanical model with state-dependent regenerative delay

Fig. 1 shows a sketch of the turning process under investigation. The tool is assumed to be compliant and experiences bending motion in directions x and y, while the workpiece is assumed to be rigid. The system can be modeled as a 2 DOF oscillator excited by the cutting force as it is shown in Fig. 2. The governing equations read

$$m\ddot{x}(t) + c_x\dot{x}(t) + k_x x(t) = F_x, \tag{1}$$

$$m\ddot{y}(t) + c_y\dot{y}(t) + k_y y(t) = F_y, \tag{2}$$

where m, c_x, c_y, k_x and k_y are the modal mass, the damping and the stiffness parameters in the x and y directions, respectively. The cutting force is given in the form

$$F_x = K_x w h^q, \tag{3}$$

$$F_y = K_y w h^q, \tag{4}$$

where K_x and K_y are the cutting coefficients, w is the depth of cut, h is the chip thickness and q is an exponent ($q = 0.75$ is a typical empirical value for this parameter). In this model, it is assumed that the tool never leaves the workpiece, that is, $h > 0$ during the cutting process.

If the tool were rigid, then the chip thickness would be a constant $h = h_0$, which is just the feed per revolution. However, in practical cases the tool experiences vibrations that alter the cutting depth and, after one revolution of the workpiece, the tool cuts this wavy surface. Thus, the regenerative effect makes the chip thickness non-constant during machining. If the regenerative delay is τ, then the chip thickness can be given as

$$h = \begin{cases} v\tau + y(t-\tau) - y(t) & \text{if } y(t) - y(t-\tau) \leqslant v\tau, \\ 0 & \text{if } y(t) - y(t-\tau) > v\tau, \end{cases} \tag{5}$$

where v is the speed of the feed. Here, the case $y(t) - y(t-\tau) > v\tau$ corresponds to the loss of contact between the tool and the workpiece. In the current work only local bifurcation

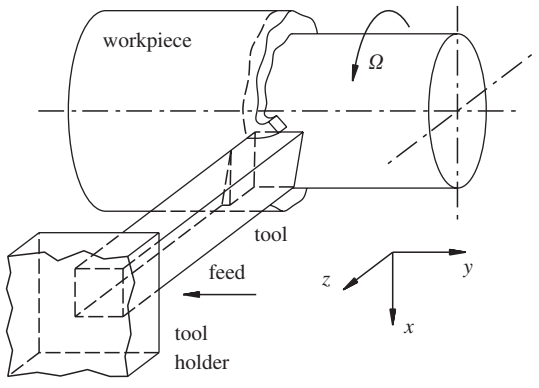

Fig. 1. Turning model.

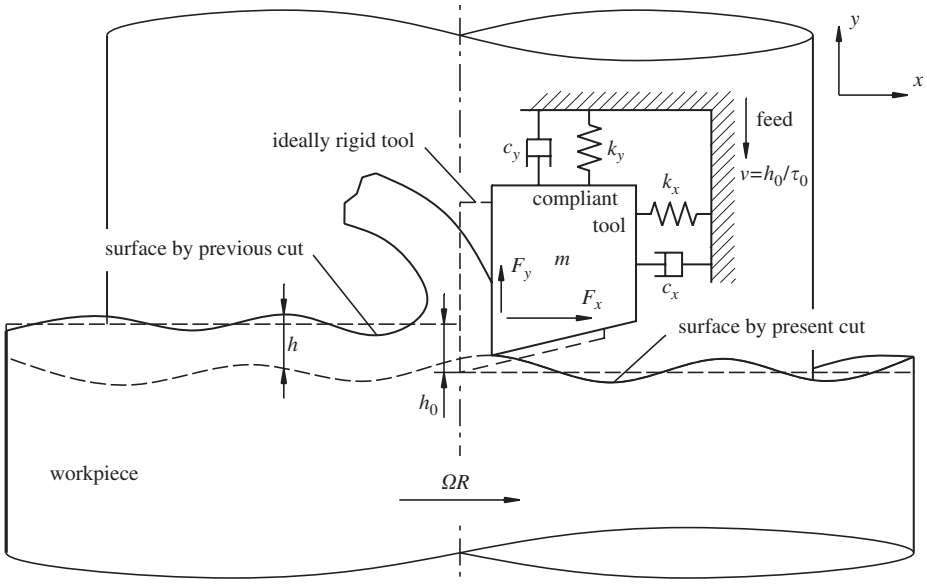

Fig. 2. Model of regeneration in turning process.

phenomena are analyzed and the effect of contact loss is not investigated. Therefore, in the following analysis, we assume that $y(t)-y(t-\tau)\leqslant v\tau$ during machining.

Since the tool experiences vibrations in the x direction as well, the time delay is not equal to the rotation period of the workpiece, but it is determined implicitly by

$$R\Omega\tau = 2R\pi + x(t) - x(t-\tau). \tag{6}$$

Here Ω is the spindle speed given in (rad/s) and R is the radius of the workpiece. Thus, the regenerative delay is a state-dependent delay since it depends on the state, both current ($x(t)$) and delayed ($x(t-\tau)$). Therefore, we will use the notation $\tau(x_t)$, where $x_t(s)=x(t+s)$, $s\in[-r,0]$, $r\in\mathbb{R}^+$ describes the history of the state.

Thus, the governing equation can be written as

$$m\ddot{x}(t)+c_x\dot{x}(t)+k_x x(t) = K_x w(v\tau(x_t)+y(t-\tau(x_t))-y(t))^q, \tag{7}$$

$$m\ddot{y}(t)+c_y\dot{y}(t)+k_y y(t) = K_y w(v\tau(x_t)+y(t-\tau(x_t))-y(t))^q. \tag{8}$$

This is a system of SD-DDEs, where the state-dependent delay $\tau(x_t)$ is given implicitly by Eq. (6).

In order to reduce the number of parameters we assume that the tool is symmetric, i.e., $c_x=c_y=c$, $k_x=k_y=k$. The corresponding natural angular frequency is $\omega_n=\sqrt{k/m}$ and the damping ratio is $\zeta=c/(2m\omega_n)$. Rescaling the state such that $x(t)=v\tau_0\tilde{x}(t)$, $y(t)=v\tau_0\tilde{y}(t)$, where $\tau_0=2\pi/\Omega$ is the mean time delay, and dropping the tildes immediately gives

$$\ddot{x}(t)+2\zeta\omega_n\dot{x}(t)+\omega_n^2 x(t) = \frac{K_x w(2\pi R)^{q-1}}{m}\rho^{q-1}\left(\frac{\tau(x_t)}{\tau_0}+y(t-\tau(x_t))-y(t)\right)^q, \tag{9}$$

$$\ddot{y}(t)+2\zeta\omega_n\dot{y}(t)+\omega_n^2 y(t) = \frac{K_y w(2\pi R)^{q-1}}{m}\rho^{q-1}\left(\frac{\tau(x_t)}{\tau_0}+y(t-\tau(x_t))-y(t)\right)^q, \tag{10}$$

where

$$\rho = v\tau_0/(2\pi R) \tag{11}$$

is the dimensionless feed rate. Note that $v\tau_0=h_0$ is the feed per revolution and $2\pi R$ is the circumference of the workpiece. Since $h_0\ll 2\pi R$, practically, $\rho\ll 1$. For instance, $\rho=0.01$ correspond to a workpiece of diameter $D=10$ mm with feed rate $h_0=0.31$ mm. Thus, in conventional turning $\rho<0.01$. Still, in the subsequent analysis, we will investigate cases with $\rho>0.01$ as well in order to point out some interesting phenomena of systems with state-dependent delay.

Rescaling now the time such that $\tilde{t}=\omega_n t$, $\tilde{\tau}=\omega_n\tau$, and $\tilde{\tau}_0=\omega_n\tau_0$, and, again, dropping the tildes immediately, yields

$$\ddot{x}(t)+2\zeta\dot{x}(t)+x(t) = \frac{1}{k_r}K_1\rho^{q-1}\times\left(\frac{\tau(x_t)}{\tau_0}+y(t-\tau(x_t))-y(t)\right)^q, \tag{12}$$

$$\ddot{y}(t)+2\zeta\dot{y}(t)+y(t) = K_1\rho^{q-1}\times\left(\frac{\tau(x_t)}{\tau_0}+y(t-\tau(x_t))-y(t)\right)^q, \tag{13}$$

where

$$K_1 = \frac{K_y w(2\pi R)^{q-1}}{m\omega_n^2} \tag{14}$$

is the dimensionless depth of cut, and $k_r = K_y/K_x$ is the cutting force ratio. Similarly, the implicit equation for the delay reduces to

$$\tau/\tau_0 = 1 + \rho(x(t) - x(t-\tau)). \tag{15}$$

Finally, the condition for the continuous cutting (i.e., without loss of contact) is

$$y(t) - y(t - \tau(x_t)) \leqslant \tau(x_t)/\tau_0. \tag{16}$$

Thus, the system under study is the SD-DDE (12)–(13) with the state-dependent delay defined by (15) and constrained by the condition (16).

If the state-dependent delay is not included into the model, then the corresponding equations are obtained by setting $\tau(x_t) = \tau_0$ in (12)–(13) and in (16). In the next sections, linear stability properties and non-linear behavior of the models with state-dependent and with constant delay are compared.

3. Linear stability

True linearization of SD-DDEs is not possible since the solution is not differentiable with respect to the state-dependent delay (see, [33] and the references therein). Linearization of SD-DDEs rather means the construction of an associated linear system that has the same local stability properties as the original system. The linearization technique for general autonomous SD-DDEs was given by Hartung and Turi [22] and for time-periodic SD-DDEs by Hartung [24].

Linear stability analysis of the SD-DDE turning problem was given in [17]. In this section, these results are summarized. The constant solution of (12)–(13) can be given as

$$\bar{x} = \frac{1}{k_r} K_1 \rho^{q-1}, \quad \bar{y} = K_1 \rho^{q-1}. \tag{17}$$

The corresponding delay is also constant: $\bar{\tau} = \tau(\bar{x}_t) = \tau_0$. The associated linearized system is

$$\ddot{\xi}(t) + 2\zeta\dot{\xi}(t) + \xi(t) = \frac{1}{k_r} K_1 q \rho^{q-1}((\eta(t-\tau_0) - \eta(t)) + \rho(\xi(t) - \xi(t-\tau_0))), \tag{18}$$

$$\ddot{\eta}(t) + 2\zeta\dot{\eta}(t) + \eta(t) = K_1 q \rho^{q-1}((\eta(t-\tau_0) - \eta(t)) + \rho(\xi(t) - \xi(t-\tau_0))). \tag{19}$$

For further details on the construction of this linear system, see [17].

Investigation of the characteristic equation gives the stability boundaries in closed form:

$$K_{1,\mathrm{SDD}} = \left(\frac{k_r}{k_r - \rho}\right) \frac{(\omega^2 - 1)^2 + (2\zeta\omega)^2}{2q\rho^{q-1}(\omega^2 - 1)}, \tag{20}$$

$$\frac{\Omega}{\omega_\mathrm{n}} = \frac{2\pi}{\tau_0} = \frac{\omega\pi}{\arctan\left(\frac{1-\omega^2}{2\zeta\omega}\right) + j\pi}, \quad j = 1, 2, \ldots, \tag{21}$$

where the Hopf frequency ω is used as a parameter, and the index SDD refers to state-dependent delay.

The stability boundaries of the corresponding system with constant time delay is

$$K_{1,\mathrm{CD}} = \frac{(\omega^2 - 1)^2 + (2\zeta\omega)^2}{2q\rho^{q-1}(\omega^2 - 1)}, \tag{22}$$

while the expression for Ω/ω_n is identical to (21). Here, the index CD refers to constant delay.

The difference between the state-dependent and the constant delay model is characterized by the ratio of the corresponding critical dimensionless depth of cut

$$\frac{K_{1,\mathrm{SDD}}}{K_{1,\mathrm{CD}}} = \frac{k_r}{k_r - \rho} > 1. \tag{23}$$

This shows that the state-dependent delay has a stabilizing effect even at the linear level. However, it should be noted that this effect is small, since $\rho \ll 1$ and typical values of the cutting force ratio are in the region of $k_r = 0.3$, so the above ratio is close to 1.

Stability boundaries in the plane $(K_1, \Omega/\omega_\mathrm{n})$ are presented in Fig. 3 for different dimensionless feed rate parameters ρ. Solid lines denote the stability boundaries associated with the state-dependent delay model, while dashed lines correspond to the constant delay model. For small feed rate ($\rho = 0.001$), the stability boundaries for the two models are practically identical, while for larger feed rates ($\rho = 0.01$ and 0.1), the difference between the two models can be seen.

In the next sections, the nonlinear behavior along the stability lobes will be investigated.

4. Bifurcation diagrams for the constant delay model

First, the main features of sub- and supercritical Hopf bifurcations are summarized. A sketch showing the amplitude of the limit cycles as a function of the dimensionless depth of cut is shown in Fig. 4 for both cases. The linear stability boundary is denoted by $K_{1,\mathrm{LSB}}$. If $K_1 < K_{1,\mathrm{LSB}}$ then the stationary cutting is stable, otherwise it is unstable. In the subcritical case, an unstable limit cycle (periodic orbit) coexists with the stable equilibrium (stationary cutting). In the supercritical case, a stable limit cycle coexists with the unstable equilibrium.

In the traditional turning models with constant regenerative delay only subcritical Hopf bifurcation occurs as was shown in [27]. This subcritical nature is clearly related to the nonlinear dependence of the cutting force on the chip thickness. For large amplitude vibrations, the tool may lose contact with the workpiece. This results in a fold back of the unstable branch to a periodic (or quasi-periodic or chaotic) attractor at $K_{1,\mathrm{FB}}$. In mechanical sense, machine tool chatter corresponds to this large amplitude attractor.

If $K_{1,\mathrm{FB}} < K_1 < K_{1,\mathrm{LSB}}$ then the large amplitude attractor coexists with the stable stationary cutting. Although the stationary cutting is linearly stable in this region, perturbations larger than the amplitude of the unstable limit cycle can still lead to chatter. Practically, the transition between stable cutting and chatter is not smooth in this case, since for a small increase of the depth of cut, large amplitude vibrations may appear suddenly.

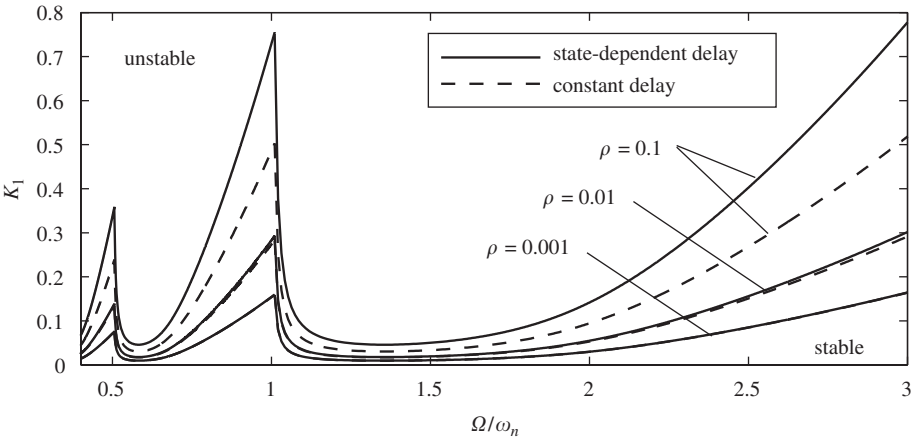

Fig. 3. Stability lobe diagrams for the state-dependent and for the constant delay models with different ρ.

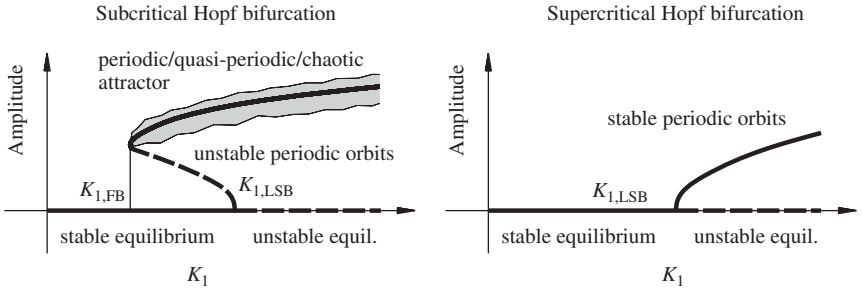

Fig. 4. Sketch of sub- and supercritical Hopf bifurcations.

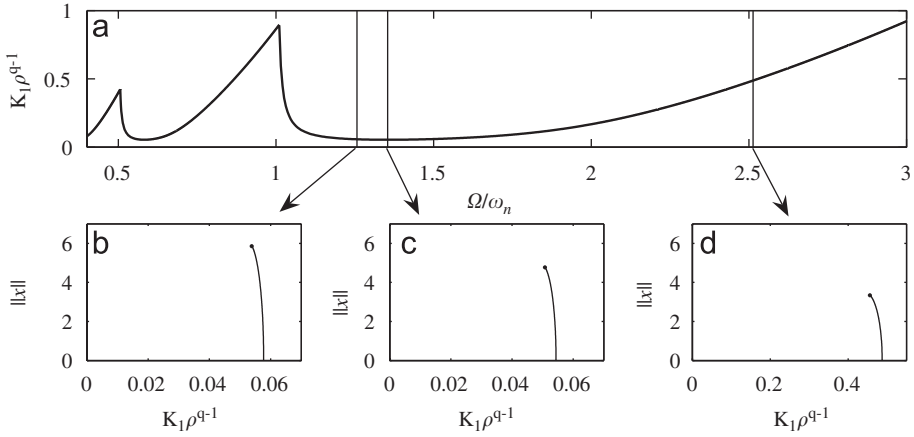

Fig. 5. Stability lobes (a) and bifurcation diagrams for the constant delay model, (b) left side of the lobe $\Omega/\omega_n = 1.2566$, (c) center of lobe $\Omega/\omega_n = 1.3541$, (d) right side of the lobe $\Omega/\omega_n = 2.5132$.

Fig. 5 shows the stability lobe diagram and three bifurcation diagrams for the constant delay model described by (12)–(13) with $\tau(x_t) = \tau_0$. Since in this case, the term ρ^{q-1} appears only as a multiplier of the dimensionless depth of cut K_1, the combined parameter $K_1\rho^{q-1}$ can be used instead of K_1 as a parameter proportional to the actual depth of cut. Thus, the bifurcation diagrams in Fig. 5 represent the amplitude of the periodic motion of the tool as function of $K_1\rho^{q-1}$ for fixed Ω/ω_n. Here, $\|x\|$ denotes the ℓ^2-norm of the displacement of the tool in the x direction:

$$\|x\| = \sqrt{\int_0^T x^2(s)\,\mathrm{d}s}, \tag{24}$$

where T is the period of the oscillation. The diagrams were determined using the software package DDE-BIFTOOL (see, [34,35]). Continuation of the periodic orbits is stopped when the continuous cutting condition (16) is broken. The points at

which the tool loses contact with the workpiece are denoted by dots in Fig. 5. It can be seen that the branches of periodic motions bends to the left for all values of ρ; these are subcritical Hopf bifurcations.

5. Non-linear analysis of the state-dependent delay model

Continuation for the system with state-dependent delay is not so straightforward as it is for the constant delay model. The software DDE-BIFTOOL can be used to the continuation of SD-DDEs, where the delay is given as explicit function of the state. However, in the model of turning, the delay is defined implicitly. To overcome this difficulty, the time delay $\tau(x_t)$ along the periodic orbit is added as an extra state variable. Thus, the time delay is given explicitly as a function of the state. To add the extra algebraic equation (15) needed to fix the time delay, DDE-BIFTOOL was modified in a similar way to the method described in [36] for continuation of neutral DDEs written as a system of DDEs coupled to an algebraic equation.

Fig. 6 shows the stability lobe diagrams and bifurcation diagrams for the state-dependent delay model with different dimensionless feed ρ. It can clearly be seen that the subcritical Hopf bifurcations change to supercritical as ρ increases. In the supercritical case, stable periodic orbits coexist with the linearly unstable stationary cutting state, while no unstable periodic orbits coexist with the stable stationary cutting state. This means that the system cannot experience chatter within the linear stability boundaries of the stationary cutting state. Also, periodic vibrations arise only when the stationary cutting state loses stability and the amplitude of these vibrations increases continuously with increasing K_1. Thus, in supercritical cases, the transition between stable cutting and chatter is smooth.

It can be seen that the criticality of the Hopf bifurcation does not change across the whole lobe. For certain spindle speeds on the left side of the lobes, when ρ is increased sufficiently, the Hopf bifurcations becomes subcritical again. However, when they become subcritical again they very quickly bend back and

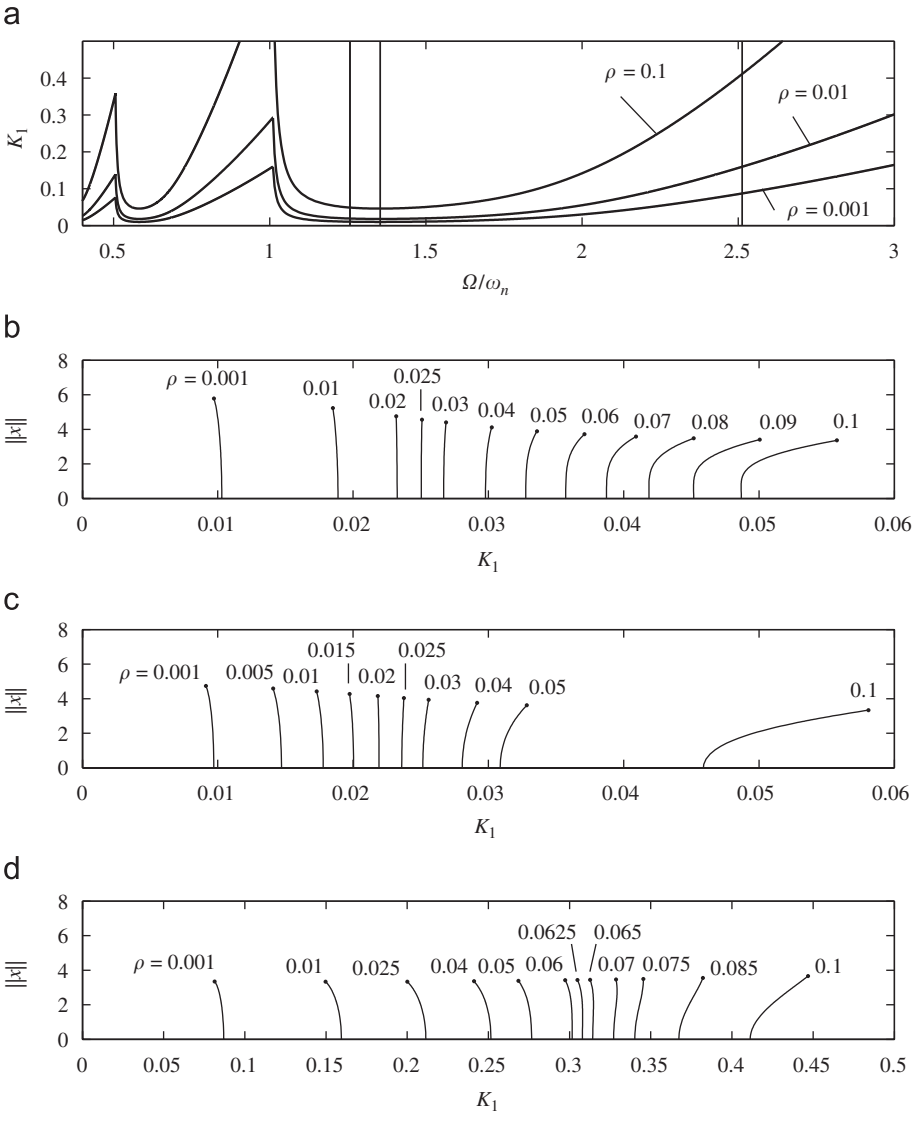

Fig. 6. Stability lobes (a) and bifurcation diagrams for the state-dependent delay model, (b) left side of the lobe $\Omega/\omega_n = 1.2566$, (c) center of lobe $\Omega/\omega_n = 1.3541$, (d) right side of the lobe $\Omega/\omega_n = 2.5132$.

so the effect is minimal. Such a case is depicted in Fig. 7; note the scale on the horizontal axis.

The transition between sub- and supercritical cases along the stability boundaries are presented in Fig. 8 for different values of the dimensionless feed ρ. The sections of the boundaries where supercritical Hopf bifurcations occur are denoted by thick lines while subcritical boundaries are denoted by thin lines. It can be seen that the right side of the lobes become supercritical for increasing ρ, while the left side remains mostly subcritical.The critical values of the dimensionless feed ρ where the criticality of the Hopf bifurcation changes are presented in Fig. 9 for the first lobe ($\Omega/\omega_n > 1$). It can be seen that there is a minimum value of the critical feed denoted by point A. The corresponding parameters are $\rho_A = 0.0209$ and $(\Omega/\omega_n)_A = 1.3225$ (it is to the left from the center of the lobe). If $\rho < \rho_A$, then

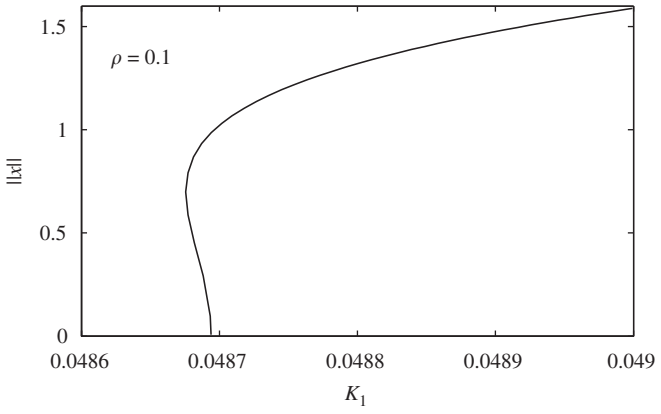

Fig. 7. Bifurcation diagram for $\Omega/\omega_n = 1.2566$, $\rho = 0.1$.

the Hopf bifurcation is always subcritical. It should be noted that ρ_A is quite large value, it corresponds to a workpiece of diameter $D = 10$ mm with feed rate $h_0 = 0.657$ mm/rev, which is not typical in practical turning.

It can also be seen that this curve bends back at point B, where $\rho_B = 0.0342$, $(\Omega/\omega_n)_B = 1.2459$. Thus, the bifurcation is also subcritical if $\Omega/\omega_n < (\Omega/\omega_n)_B$.

In Fig. 9 only the first lobe is considered but this phenomenon is the same for all the other lobes as is seen from the parameterization of (21). Assume that $\omega = \omega_{cr}$ is the chatter frequency, where the criticality of the bifurcation changes in the first lobe. In this case, the period of the limit cycles arising from the Hopf bifurcation is $T_{cr} = 2\pi/\omega_{cr}$. Using (21) with $j = 1$, the corresponding time delay is

$$\tau_{01} = \frac{2\arctan\left(\frac{1-\omega_{cr}^2}{2\zeta\omega_{cr}}\right) + 2\pi}{\omega_{cr}}. \tag{25}$$

For any other lobes with $j = n > 1$, $\omega = \omega_{cr}$ gives the delay

$$\tau_{0n} = \frac{2\arctan\left(\frac{1-\omega_{cr}^2}{2\zeta\omega_{cr}}\right) + n2\pi}{\omega_{cr}}. \tag{26}$$

Note, that $\tau_{0n} - \tau_{01} = (n-1)2\pi/\omega_{cr} = (n-1)T_{cr}$. Now, we can say that if $\hat{x}(t) = \hat{x}(t + T_{cr})$ is a periodic solution of the system with time delay $\tau = \tau_{01}$, then it is also the solution for the system with $\tau = \tau_{0n}$, since

$$\hat{x}(t - \tau_{01}) = \hat{x}(t - \tau_{01} - (n-1)T_{cr}) = \hat{x}(t - \tau_{0n}). \tag{27}$$

This means that the criticality of the bifurcation changes at the chatter frequency $\omega = \omega_{cr}$ for all the lobes.

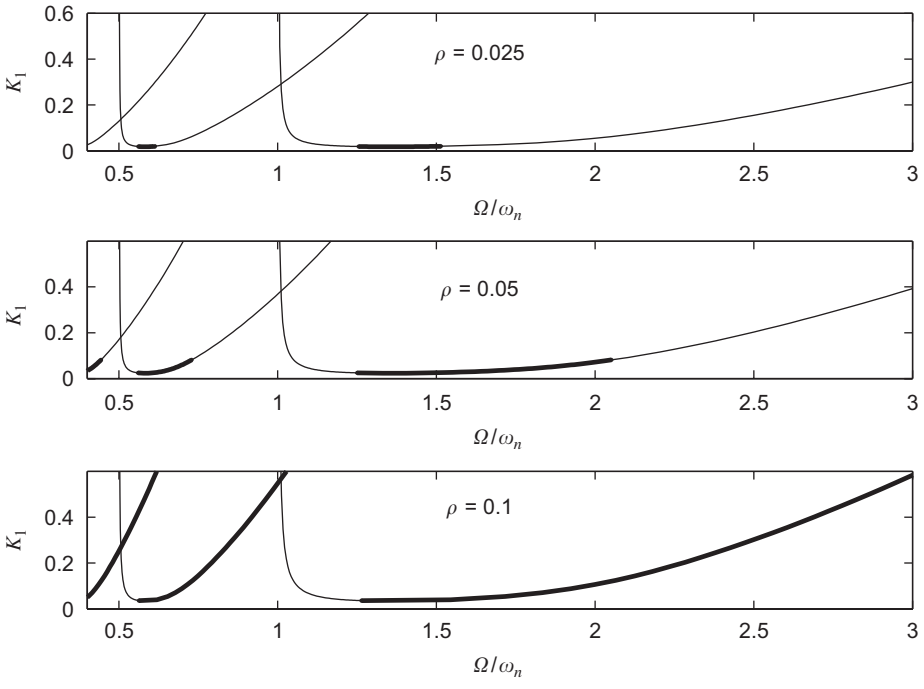

Fig. 8. Change of criticality along the lobes. Thick lines—supercritical, thin lines—subcritical.

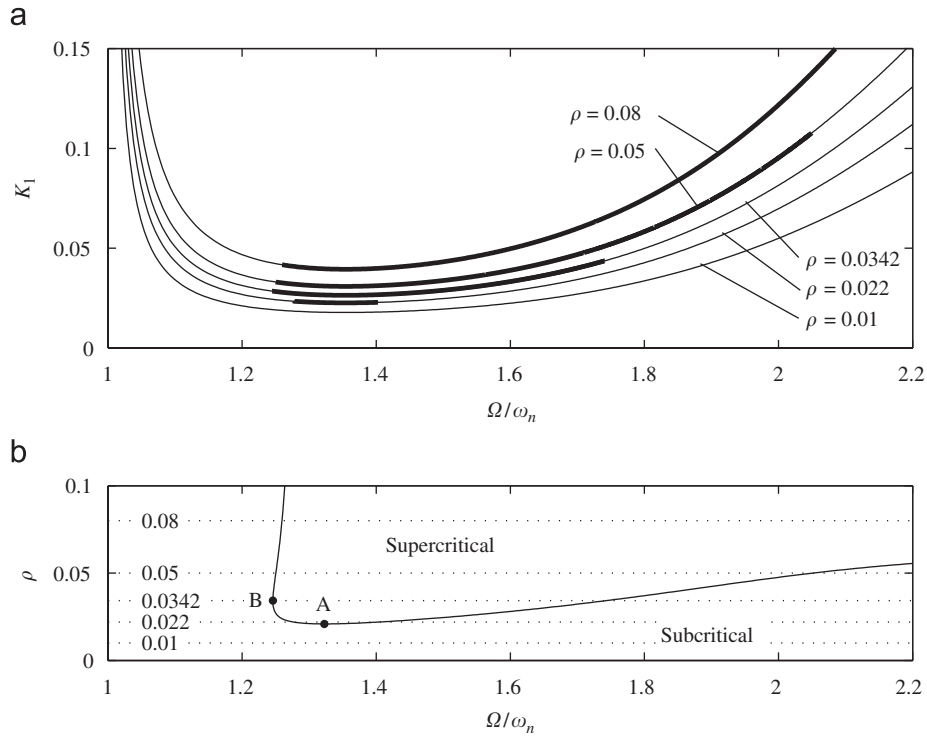

Fig. 9. Change of criticality along the first lobe (a), thick lines—supercritical, thin lines—subcritical. Criticality chart (b).

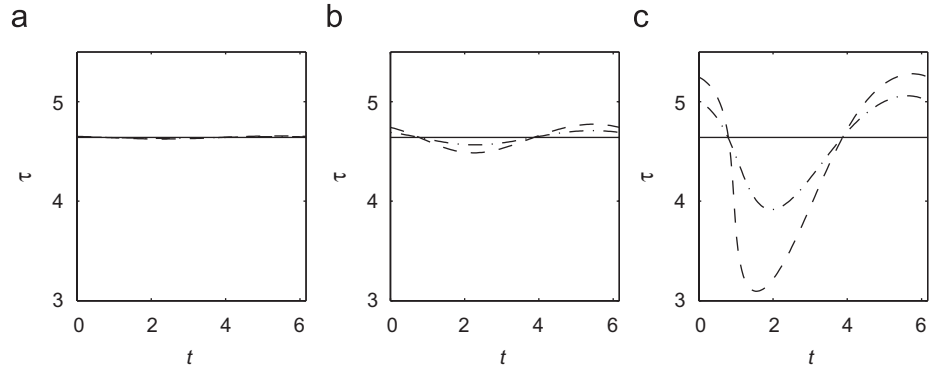

Fig. 10. Variation of the time delay at the minimum of the lobe ($\Omega/\omega_n = 1.3541$) for $\rho = 0.001$ (a), $\rho = 0.01$ (b) and $\rho = 0.1$ (c). Solid lines—close to the Hopf bifurcation, dashed lines—close to loss of contact, dash-dot lines—middle of the branches.

Fig. 10 shows the variation of the time delay along the periodic branches at the center of the lobe ($\Omega/\omega_n = 1.3541$). In order to be able to compare the variations in the time delays, the periods of the orbits are normalized to 2π. It can be seen that the amplitude of the delay variation increases with the dimensionless feed ρ. Also, the assumption of a constant delay as made by previous DDE models is clearly flawed.

6. Conclusion

The non-linear dynamics of the state-dependent delay model of turning processes was analyzed using numerical continuation methods. The important difference between this model and other models is that the regenerative delay is determined not just by the rotation of the workpiece, but also by the vibrations of the tool. The linear stability analysis of the model was given earlier in [17], where it was shown that the stability lobes associated with the state-dependent delay model are slightly higher than those of the constant delay model.

The mathematical model is an SD-DDE where the time delay is defined implicitly. The behavior of the system at the linear stability boundaries was investigated. Specifically, the criticality of the Hopf bifurcation at the stability loss was determined. A modified version of DDE-BIFTOOL was used that allows the time delay to be treated as an extra state variable. The analysis showed that the criticality of the Hopf bifurcations along the stability lobes depends on the feed rate. For small feed rates, the bifurcation is subcritical, similarly to the models with

constant spindle speed (see [27]). In this case, an attractor (either a periodic or quasi-periodic orbit, or a chaotic attractor) coexists with the stable stationary cutting state that may lead to chatter even within the linear stability boundaries. For large feed rates, it was found that the bifurcation becomes supercritical for certain spindle speeds, mostly on the right-hand side of the stability lobe. In the supercritical case, stable periodic orbits coexist with the linearly unstable stationary cutting state, and no attractors coexist with the stable stationary cutting state. This means that the system cannot experience chatter within the linear stability boundaries. From practical point of view, clearly, the supercritical Hopf bifurcation is more favorable than the subcritical one. Adaptive chatter control strategies [37] are also much more efficient at supercritical stability boundaries.

Thus, it was shown that the state-dependent delay in the turning model has a kind of stabilizing effect. It increases the linear stability limits and it turns the subcritical bifurcations to supercritical ones. In some respect, the state-dependent time delay has a kind of compliance compared to the "stiff" constant delay. As a rule of thumb, we might say that the more flexible the delay is, the more stable the system is.

The fact that varying regenerative delay may stabilize cutting processes is well known in the machining community. This is the goal when varying spindle speeds are applied, or milling tools with variable pitch angles are used. However, in these cases, the variation in the delay is prescribed, while in the cases of state-dependent delays, it is self-regulated.

Acknowledgments

The authors acknowledge the support from the Centre de Recerca Matemàtica (CRM), Barcelona, Thematic Research Term on Non-Smooth Complex Systems. T.I. was supported by the János Bolyai Research Scholarship of the Hungarian Academy of Sciences and the Hungarian National Science Foundation under Grant no. OTKA F047318. D.A.W.B. is a research fellow supported by the Lloyds Tercentenary Foundation. G.S. was supported by the Hungarian National Science Foundation under Grant no. OTKA T068910.

References

[1] J. Richard, Time-delay systems: an overview of some recent advances and open problems, Automatica 39 (10) (2003) 1667–1694.
[2] B. Krauskopf, Unlocking dynamical diversity: optical feedback effects on semiconductor lasers, in: D. Kane, K. Shore (Eds.), Bifurcation Analysis of Lasers with Delay, Wiley, New York, 2005, pp. 147–183.
[3] M. Breakspear, J. Roberts, J. Terry, S. Rodrigues, N. Mahant, P. Robinson, A unifying explanation of primary generalized seizures through nonlinear brain modeling and bifurcation analysis, Cerebral Cortex 16 (9) (2006) 1296–1313.
[4] J. Tlusty, A. Polacek, C. Danek, J. Spacek, Selbsterregte Schwingungen an Werkzeugmaschinen, VEB Verlag Technik, Berlin, 1962.
[5] S.A. Tobias, Machine Tool Vibration, Blackie, London, 1965.
[6] J. Hale, S. Verduyn Lunel, Introduction to Functional Differential Equations, Springer, New York, 1993.
[7] O. Diekmann, S. van Gils, S. Verduyn Lunel, H.-O. Walther, Delay Equations: Functional-, Complex-, and Nonlinear Analysis, Springer, New York, 1995.
[8] G. Stépán, Retarded Dynamical Systems, Longman, Harlow, 1989.
[9] Y. Altintas, E. Budak, Analytical prediction of stability lobes in milling, Ann CIRP 44 (1) (1995) 357–362.
[10] B. Balachandran, M.X. Zhao, A mechanics based model for study of dynamics of milling operations, Meccanica 35 (2) (2000) 89–109.
[11] T. Insperger, B.P. Mann, G. Stépán, P.V. Bayly, Stability of up-milling and down-milling. Part 1: alternative analytical methods, Int. J. Mach. Tools Manuf. 43 (1) (2003) 25–34.
[12] S.D. Merdol, Y. Altintas, Multi frequency solution of chatter stability for low immersion milling, J. Manuf. Sci. Eng. 126 (3) (2004) 459–466.
[13] X.-H. Long, B. Balachandran, Milling model with variable time delay, in: Proceedings of the 2004 ASME International Mechanical Engineering Congress and Exposition, Anaheim, CA, paper no. IMECE2004-59207, 2004.
[14] R.P.H. Faassen, N. van de Wouw, H. Nijmeijer, J.A.J. Oosterling, An improved tool path model including periodic delay for chatter prediction in milling, J. Comput. Nonlinear Dyn. 2 (2007) 167–179.
[15] X.-H. Long, B. Balachandran, B.P. Mann, Dynamics of milling processes with variable time delay, Nonlinear Dyn. 47 (2007) 49–63.
[16] T. Insperger, G. Stépán, J. Turi, State-dependent delay model for regenerative cutting processes, in: Fifth EUROMECH Nonlinear Dynamics Conference, ENOC 2005, Eindhoven, The Netherlands, 2005, pp. 1124–1129.
[17] T. Insperger, G. Stépán, J. Turi, State-dependent delay in regenerative turning processes, Nonlinear Dyn. 47 (1–3) (2007) 275–283.
[18] C. Germay, N. van de Wouw, R. Sepulchure, H. Nijmeijer, Axial stick-slip limit cycling in drill-string dynamics with delay, in: Fifth EUROMECH Nonlinear Dynamics Conference, ENOC 2005, Eindhoven, The Netherlands, 2005, pp. 1136–1143.
[19] T. Richard, C. Germay, E. Detournay, A simplified model to explore the root cause of stick-slip vibrations in drilling systems with drag bits, J. Sound Vib. 305 (2007) 432–456.
[20] T. Insperger, G. Stépán, F. Hartung, J. Turi, State-dependent regenerative delay in milling processes, in: Proceedings of ASME International Design Engineering Technical Conferences, Long Beach CA, paper no. DETC2005-85282, 2005.
[21] I. Győri, F. Hartung, On the exponential stability of a state-dependent delay equation, Acta Sci. Math. 66 (2000) 71–84.
[22] F. Hartung, J. Turi, Linearized stability in functional–differential equations with state-dependent delays, in: Proceedings of the conference Dynamical Systems and Differential Equations added volume of Discrete and Continuous Dynamical Systems, 2000, pp. 416–425.
[23] T. Luzyanina, K. Engelborghs, D. Roose, Numerical bifurcation analysis of differential equations with state-dependent delay, Int. J. Bifurcation Chaos 11 (3) (2001) 737–753.
[24] F. Hartung, Linearized stability in periodic functional differential equations with state-dependent delays, J. Comput. Appl. Math. 174 (2005) 201–211.
[25] F. Hartung, T. Krisztin, H.-O. Walther, J. Wu, Functional differential equations with state-dependent delay: theory and applications, in: A. Canada, P. Drbek, A. Fonda (Eds.), Handbook of Differential Equations: Ordinary Differential Equations, vol. 3, Elsevier, North-Holand, 2006, pp. 435–545.
[26] H.M. Shi, S.A. Tobias, Theory of finite amplitude machine tool instability, Int. J. Mach. Tool Des. Res. 24 (1984) 45–69.
[27] G. Stépán, T. Kalmár-Nagy, Nonlinear regenerative machine tool vibration, in: Proceedings of the 1997 ASME Design Engineering Technical Conferences, Sacramento, California, paper no. DETC97/VIB-4021, 1997.
[28] T. Kalmár-Nagy, J.R. Pratt, M.A. Davies, M. Kennedy, Experimental and analytical investigation of the subcritical instability in metal cutting, in: Proceedings of the 1999 ASME Design Engineering Technical Conferences, Las Vegas, Nevada, paper no. DETC99/VIB-8060, 1999.
[29] P. Wahi, A. Chatterjee, Regenerative tool chatter near a codimension 2 Hopf point using multiple scales, Nonlinear Dyn. 40 (2005) 323–338.
[30] P. Wahi, A study of delay differential equations with applications to machine tool vibrations, Ph.D. Thesis, Indian Institute of Science, Bangalore, 2005.
[31] N.K. Chandiramani, T. Pothala, Dynamics of 2-dof regenerative chatter during turning, J. Sound Vibration 290 (2006) 448–464.

[32] Z. Dombóvári, R.E. Wilson, G. Stépán, Large amplitude nonlinear vibrations in turning processes, in: Sixth International Conference on High Speed Machining, San Sebastian, Spain, 2007.

[33] F. Hartung, J. Turi, On differentiability of solutions with respect to parameters in state-dependent delay equations, J. Differential Equations 135 (2) (1997) 192–237.

[34] K. Engelborghs, T. Luzyanina, G. Samaey, DDE-BIFTOOL v. 2.00: a Matlab package for bifurcation analysis of delay differential equations, Technical Report TW-330, Department of Computer Science, K.U. Leuven, Leuven, Belgium, 2001.

[35] K. Engelborghs, T. Luzyanina, D. Roose, Numerical bifurcation analysis of delay differential equations using DDE-BIFTOOL, ACM Trans. Math. Software 28 (1) (2002) 1–21.

[36] D.A.W. Barton, B. Krauskopf, R.E. Wilson, Collocation schemes for periodic solutions of neutral delay differential equations, J. Difference Equations Appl. 12 (11) (2006) 1087–1101.

[37] R.P.H. Faassen, Chatter prediction and control for high-speed milling: modelling and experiments, Ph.D. Thesis, Eindhoven University of Technology, Eindhoven, Netherland, 2007.